Available online at www.sciencedirect.com
SCIENCE DIRECT®
International Journal of Heat and Mass Transfer 49 (2006) 1592–1602
International Journal of HEAT and MASS TRANSFER
www.elsevier.com/locate/ijhmt

Adiabatic water absorption properties of an aqueous absorbent at very low pressures in a spray absorber

F.S.K. Warnakulasuriya, W.M. Worek *

Department of Mechanical and Industrial Engineering, 842 West Taylor Street, University of Illinois at Chicago, Chicago, IL 60607-7022, United States

Received 7 November 2005; received in revised form 11 November 2005
Available online 20 January 2006

Abstract

In this paper, spray absorber in absorption chillers, a new technique is proposed. This concept of atomization increases the heat and mass transfer rates due to the increases of the expose area of the brine solution compared to falling film technique used in the conventional absorber. Results presented in this paper show the great enhancement of water absorption property by having a pressure atomization. The experimental set up was included a single nozzle adiabatic spray chamber operating at the design pressure, a solution circulating and tempering system, a Laser measurement system to measure the size and the velocity of the droplets, and data acquisition and control system. Based on a first principle ''Newman model'', an analytical model was developed to predict the enhance transfer rates. These analytical results were compared with the experimental results that showed good agreement. The experiments were conducted by varying the differential pressure across the nozzle and the liquid desiccant flow rate. The dimensionless viscosity ratio, k, of this disperse/continuous phase flow was around 1300. The nozzles tested were able to produce the expected drop sizes and mean drop velocities. The droplet Reynolds number and Peclet number varied from 10 to 1500 and 0.005 to 0.5, respectively.

Keywords: Absorption refrigeration; Drop absorption; Spray in low-pressure environment; Absorber model; Drop measurement

1. Introduction

In multi-effect high-performance absorption cycle chillers, the high temperature loops operate with highly concentrated salt solutions that are relatively viscous and corrosive. Consequently, the design of corresponding apparatus, especially the absorber, presents engineering and material challenges. Current absorber designs are large which affects the size and the cost of absorption chillers. Therefore, any improvement in the effectiveness of an absorber would reduce the size of the absorber and consequently the system. This could enable absorption systems to be smaller and more compact.

In the development of new multi-effect absorption chillers, the possibility of using new absorbents, in this case LZB™ by ''Trane Company'' which is essentially a lithium-based liquid absorbent, which meets new operating conditions, as well as use of mass transfer enhancement techniques are being investigated. One conceptual technique to enhance the transport rates is the concept of spray absorption.

In an absorber, the most important parameter is the rate the refrigerant (in this case, it is water) in the form of vapor is absorbed by the concentrated salt solution. It has been recognized that if this rate could be increased, as compared to conventional absorbers, the energy consumption and the size of the absorber and hence the cost could be reduced.

It is apparent that if the total absorption area of the salt solution could be increased, the rate of water vapor absorption would proportionally be increased. One way of doing this is to introduce the absorption fluid in the form of the fine droplets, which could increase the absorption rate. It is known that as the size of these droplets decreases, the total area exposed to the vapor increases and the rate of absorption increases accordingly. Benberhim et al. [1],

* Corresponding author. Fax: +1 312 413 0447.
E-mail address: wworek@uic.edu (W.M. Worek).

0017-9310/$ - see front matter © 2005 Elsevier Ltd. All rights reserved.
doi:10.1016/j.ijheatmasstransfer.2005.11.003

Nomenclature

a	radius of drop, m (ft)
A_l	local absorption rate, mol/m^2 s (mol/ft^2 min)
D	diameter of the drop, m (ft)
F	F factor, fractional approach to equilibrium
h	enthalpy, kJ/kg (Btu/lb$_m$)
h_m	a surface mass transfer coefficient, m/s (ft/min)
k	viscosity ratio = viscosity of disperse phase/viscosity of continuous phase
K_D	Fick's diffusion coefficient or chemical diffusivity (mass diffusivity), m^2/s (ft^2/min)
$\dot{m}$	solution mass flow rate, kg/s (lb$_m$/min)
Pe	mass transfer Peclet number = UD/K_D
Re	Reynolds number = UD/ν
r	radial direction variable, m (ft)
Sh_p	the global particle Sherwood number (the instantaneous overall Sherwood number)
t	resident time of drops, s
u	directional velocity component, m/s (ft/min)
U	speed of the drop, m/s (ft/min)
X	solution concentration mol water/m^3 solution (mol water/ft^3 solution)
X_i	interface solution concentration. This is also the ultimate equilibrium concentration that the drop ultimately reaches as dimensionless time factor, τ, goes to infinity, mol/m^3 (mol/ft^3)
X_m	mean or bulk solution concentration, mol/m^3 (mol/ft^3)
X_0	initial concentration at the nozzle, mol/m^3 (mol/ft^3)
$(\partial\rho/\partial\Delta)$	effect of the error on the ultimate calculation, in this paper, the effect of the error on the absorption ratio

Greek symbols

θ	horizontal tangential direction variable
τ	dimensionless time factor similar to Fourier number
Δ	error of some particular reading
ν	kinematic viscosity

Subscripts

s	salt portion of the spray
w	water portion of the spray
v	water vapor absorbed
o	at the nozzle (inlet)
f	at ultimate equilibrium

Summerer et al. [2], Morioko et al. [3] and Ryan [4] confirmed the above effects with experiments, analytical and numerical calculations. Those studies show that replacing a conventional absorber with a spray absorber and enhancing the mass transfer process is practically feasible. The conceptual comparison of the processes of above two absorbers can be seen in Fig. 1.

The main objective of this work is to find the water absorption quality of the absorbent under different operating conditions. In addition, the results of this research will indicate the best nozzle types to be used in commercial applications, and the optimum operating conditions for those selected nozzles. To meet the above objectives, comparison studies between the experimental results and analytical results based on existing first principal "Newman" model is presented.

2. Drop absorption

In the spray absorber, if the solution is at equilibrium, the vapor pressure is lower than the water vapor pressure, the solution is sub-cooled, and it will absorb water vapor. During the absorption process, the solution will become dilute and due to the heat evolved, the temperature will increase until the equilibrium pressure has increased to the absorber pressure. After this point, no further absorption will occur. The above process can be easily explained by an equilibrium chart or a Duhring diagram for the salt solution [5].

The main factors that affect the water absorption into sub-cooled solution droplets are the level of sub-cooling, the chemical diffusivity, the droplet resident time, the internal fluid motion within the droplet (i.e., the Marangoni effect) and the capillary pressure. Since the mean diameter of the droplets is in order of 400 μm, the effect form the capillary pressure is negligible [4,5].

Over the last 70 years, numerous authors including Newman [6], Higbie [7], Kronig and Brink [8], Handlos and Baron [9], Rose and Kintner [10], Grigor'eva and Nakoryakov [11,12], and Ruckenstein [13] have studied and modeled absorption processes in falling drops assuming different flow conditions.

In the above first principle theoretical models of the falling drop absorption, the species conservation equation is,

$$\frac{\partial X}{\partial t} = K_D \nabla^2(X). \tag{1}$$

This equation can be expanded adding convective terms in spherical coordinates for the surface composition of particles undergoing unsteady mass transfer with negligible external resistance. Therefore, Eq. (1) becomes

$$\frac{\partial X}{\partial t} + u_r \frac{\partial X}{\partial r} + \frac{u_\theta}{r}\left(\frac{\partial X}{\partial \theta}\right) = \frac{K_D}{r^2}\left[\frac{\partial}{\partial r}\left(r^2 \frac{\partial X}{\partial r}\right)\right] + \frac{1}{\sin\theta}\left[\frac{\partial}{\partial \theta}\left(\sin\theta \frac{\partial X}{\partial \theta}\right)\right]. \tag{2}$$

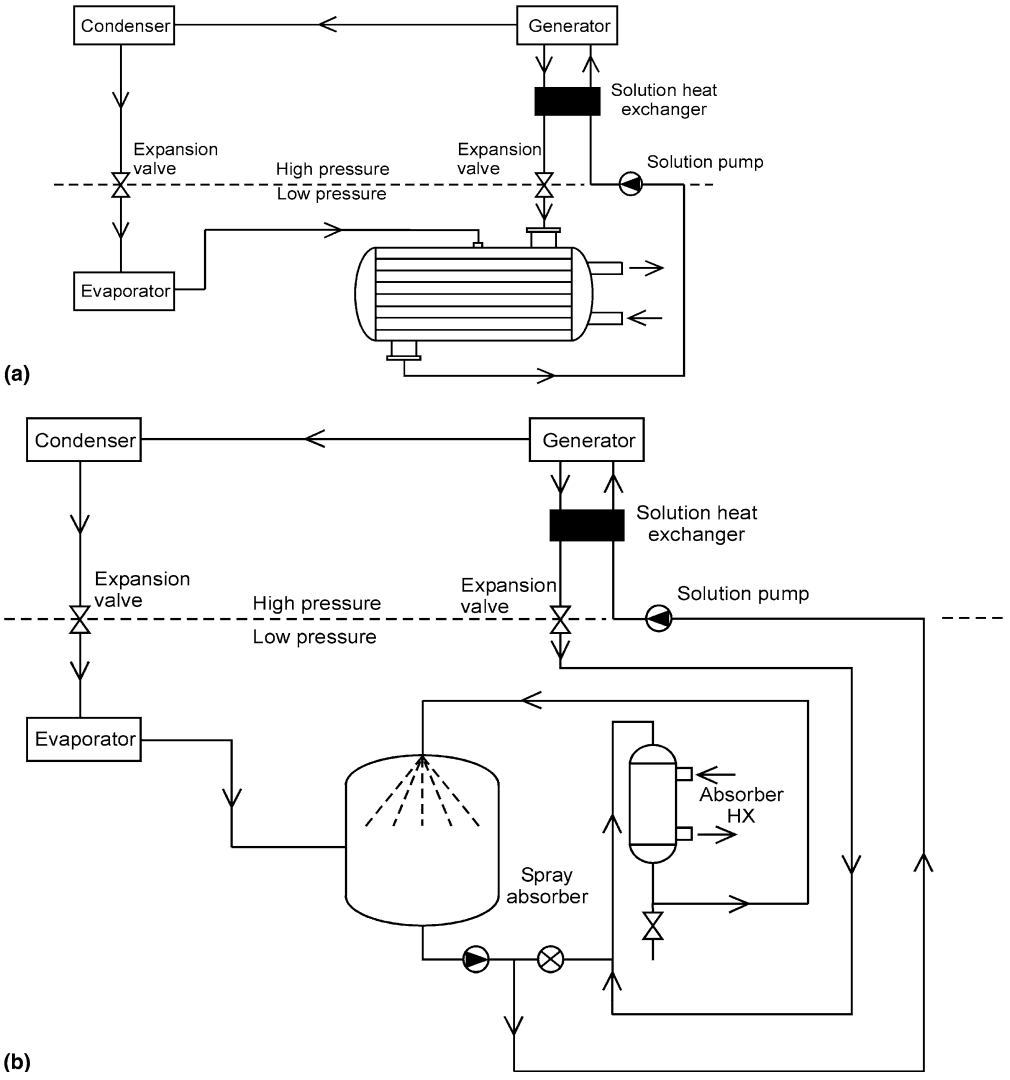

Fig. 1. Conventional absorber (above) and spray absorber with solution sub-cooler (below).

Where the vertical tangential direction variable is negligible, since the tangential velocity component is negligible. The most general boundary condition for this type of flow model is

$$X = X_{\mathrm{i}} \quad \text{at } r = a. \tag{3}$$

This boundary condition assumes that the interface immediately reaches the equilibrium condition, X_{i}, which is ultimately experienced by the entire drop. Clifts [14] described that this assumption follows the pattern established by previous investigators and allows decoupling the temperature and the concentration equations.

The second boundary condition is

$$\frac{\partial X}{\partial r} = 0 \quad \text{at } r = 0. \tag{4}$$

The initial condition is simply specified as

$$X = X_0 \quad \text{at } t = 0 \text{ at any } r. \tag{5}$$

The most useful properties that can be calculated using above equation and boundary conditions are local absorption rate, A_{i}, given by

$$A_{\mathrm{l}} = K_{\mathrm{D}} \left(\frac{\partial X}{\partial r} \right)_{r=a}, \tag{6}$$

and the mass transfer coefficient, h_{m}, which depends on the absorption rate, given by

$$A_{\mathrm{l}} = h_{\mathrm{m}} (X_{\mathrm{i}} - X_{\mathrm{m}}). \tag{7}$$

In order to derive an expression for the local absorption rate, the dimensionless form of above governing equation has to be considered. It is convenient to define the dimensionless concentration or fractional approach to equilibrium, F factor as,

$$F = \frac{(X_{\mathrm{m}} - X_0)}{(X_{\mathrm{i}} - X_0)}. \tag{8}$$

The driving force is taken as the difference between the concentration inside the interface, X_{i}, and the mean particle

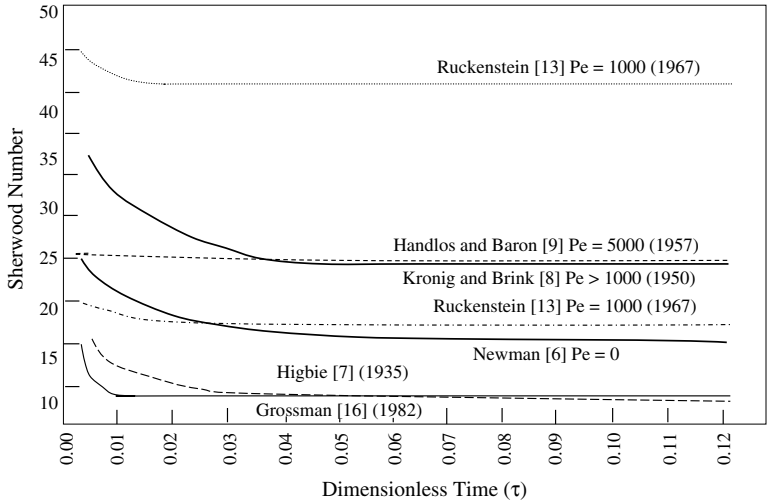

Fig. 2. Comparison of F verses τ for different drop absorption models.

concentration, X_m. The relationship of the above solutions to the governing equation can be found in [15].

The sprays investigated in this work were largely non-oscillating and have low Peclet numbers [15]. Therefore, the oscillation and internal turbulence are not important factors. For this case, only the "Newman" model is appropriate under above conditions. Comparison of the Sherwood number (dimensionless concentration gradient) for above mentioned widely accepting drop absorption models are given in Fig. 2. These plots are for drops with 300-μm drop diameter. The line marked "Grossman (1982)" [16] in Fig. 2 is for typical 300 μm thick adiabatic laminar falling film occurring in the conventional absorber. The comparison of plots show the Sherwood number for drops can be far higher than that for the laminar falling-film.

3. Newman model

When mass diffuses into a fluid particle, the concentration within the particle changes with time. The concentration fields for both internal and external fluids are related to the interface. If there is no chemical reaction at the interface, the species mass fluxes on each side are equal. If the Peclet number of a drop flow is small (i.e., $Pe \cong Pe_s \cong 0$), the external resistance is negligible and hence, internal motion of the fluid within the drop can be ignored. Therefore, the concentration profiles display angular symmetry. Further, the fractional approach to equilibrium, F, is a function only of diffusivity and the dimensionless time number. With these bases for the Newman absorption model [6], it is possible to simplify the species conservation equation (2), considering $u_r = u_\theta = 0$ gives

$$\frac{\partial X}{\partial \tau} = \frac{K_D}{r^2}\left[\frac{\partial}{\partial r}\left(r^2\frac{\partial X}{\partial r}\right)\right] = \frac{K_D}{r}\left[\frac{\partial^2}{\partial r^2}(rX)\right]. \tag{9}$$

Eq. (9) was solved by Newman, with boundary and initial conditions as in Eqs. (3)–(5), to a series solution as

$$F = 1 - \left\{\frac{6}{\pi^2}\sum_{n=1}^{\infty}\left[\frac{\exp(-n^2\pi^2\tau)}{n^2}\right]\right\} \tag{10}$$

and

$$Sh_p = \frac{2\pi^2}{3}\frac{\sum_{n=1}^{\infty}\exp(-n^2\pi^2\tau)}{\sum_{n=1}^{\infty}\frac{1}{n^2}\exp(-n^2\pi^2\tau)}. \tag{11}$$

4. The thermodynamic model

As the absorption occurs rapidly and the surrounding pressure exerted by the water vapor is very low, the absorption process can be considered as adiabatic. If drops are falling down in the absorber for an infinite amount of time, the concentration change in the absorber is $X_i - X_0$. However, real sprays have finite drop lifetimes. The above Newman model calculates the fractional approach equilibrium, F, expected over the actual lifetime of the drops.

Therefore, the actual concentration change through a real absorber is given as,

$$\Delta X_{\text{actual}} = F(X_i - X_0). \tag{12}$$

In order to find the actual concentration changes in the absorber chamber, in addition to the factor F, the values for X_i (i.e., the ultimate equilibrium concentration) must be known. Since both the ultimate enthalpy and concentration are unknown, the process of finding the valves for X_i is based on thermodynamics analysis.

Considering species energy conservation equation and curve fit equations for the Duhring diagram and enthalpy chart [5], Warnakulasuriya [17] found solutions for the above two unknowns, iteratively.

As the spray comes to the equilibrium adiabatically, energy conservation dictates that,

$$m_0h_0 + m_vh_v = m_fh_f = (m_0 + m_v)h_f. \tag{13}$$

Rearranging Eq. (13) gives,

$$m_v = m_0 \left\{ \frac{h_f - h_0}{h_v - h_f} \right\}. \quad (14)$$

Eq. (14) together with enthalpy data can be used to solve the two unknowns, m_v and h_f. However, generally absorption equipment manufacturers use the salt solution weight percentage to characterize the properties of solutions. Therefore, expressing the energy conservation equation by chemical species gives,

$$(m_{s_0} + m_{w_0})h_0 + m_v h_v = (m_{s_f} + m_{w_f})h_f, \quad (15)$$

and from the conservation of species,

$$m_{s_0} = m_{s_f} \quad m_{w_0} + m_v = m_{w_f}. \quad (16)$$

As $Wt\%_{inlet} = m_{s_0}/m_0$, from above equation, the $Wt\%_{final}$ of salt solution at the exit can be defined as,

$$Wt\%_{final} = \left(\frac{1}{1 + \frac{h_f - h_0}{h_v - h_f}} \right) Wt\%_{inlet}. \quad (17)$$

In above equations, the $Wt\%_{final}$ is the weight present of salt in solution as it leaves the absorber, and $Wt\%_{inlet}$ is weight present of salt in solution as it enters the absorber.

The above analysis solves the equation for solution concentration at ultimate equilibrium with the vapor, the enthalpy, h_f, and concentration, X_i, of the solution if the solution is brought to equilibrium adiabatically.

Similarly, in order to define the rate of water vapor absorbed by the salt solution in single pass, the absorber manufacturing industry use the term absorption ratio, which can be defined as

$$\text{Absorption ratio} = \frac{\text{Weight of water vapor absorbed}}{\text{Unit weight of circulated salt solution}}. \quad (18)$$

5. Experimental setup

The design and construction of the experimental setup was intended to obtain the required operating conditions as well as to obtain experimental values required to calculate the experimental absorption rates, the model absorption rates and the experimental and predicted absorption ratios. In addition, this test setup should produce a reproducible spray using commercially available spray nozzles (manufactured by Spraying System Incorporated), allow a high degree of accuracy in the measurement of absorption rate, solution temperature and absorber pressure, and provide a good visibility of the spray process for observation and laser measurement of drop sizes and velocities. The required ranges of operating parameters are as given in Table 1.

The nozzle pressure of any particular test depended on the development of the spray for that specific nozzle and the maximum spray angle that any spray can reach before contact with the absorber chamber wall, due to the limited diameter of the chamber.

Based on the previous studies performed by industry nozzle manufacturers and previous experiments related to this research by Warnakulasuriya [17], whirl jet and full jet nozzles were selected for the experiments. Based on the spray of water at 6.89×10^4 Pa (10 psig) nozzle pressure, the manufacturer's specification of all nozzles tested are given in Table 2.

The schematic diagram of the mass transfer test setup is shown in Fig. 3. In order to facilitate the required pressure differences across the nozzle and to maintain the exact pressure inside the absorber chamber, a high vacuum system that includes diffusion pump and two 20-l/min vacuum pumps were used. This system was able to maintain a pressure of 25 Pa with the leakage rate of 4.67×10^{-6} std cm^3/s.

For the drop size and velocity measurements, an Aerometric Phase Doppler Particle Analyzer (PDPA) was used. This instrument is capable of simultaneously measuring both drop size and velocity.

First, using the results obtained from vapor flow measurements for each nozzle, absorption rates purely based on experimental results at different sub-cooled levels and different nozzle pressures were analyzed. Second, using the experimental results obtained to calculate the model results for each nozzle tested, the absorption rates and absorption ratios using the computer program based on

Table 1
Operating conditions

Parameter	Range
Required concentration of salt solution at nozzle	84% by weight
Required nozzle pressure range	0–1.7×10^5 Pa (0–10 psig)
Required absorber pool temperature	92.2 °C (198 F)
Required solution temperature range at nozzle	65.5–82.2 °C (150–180 F)
Required absorber pressure	1.23 kPa (9.24 mm Hg)

Table 2
Nozzle specification

Type	Model	Droplet size (water) [MVD $\times 10^6$ m^{-1}]	Capacity (water) [$Q \times 10^6$ m^{-3} s^{-1} (Q gpm^{-1})]	Spray angle [deg]
Whirl jet	1/8 BX SS 1	252	6.3×10^{-6} (0.10)	52
Whirl jet	1/8 BX SS 2	263	1.2×10^{-5} (0.20)	54
Whirl jet	1/8 BX SS 2W	268	1.6×10^{-5} (0.25)	114
Whirl jet	1/8 BX SS 3	275	1.9×10^{-5} (0.30)	56
Full jet	1/8 GG SS 2	325	1.2×10^{-5} (0.20)	43
Full jet	1/8 GG SS 2.8W	338	1.8×10^{-5} (0.28)	120

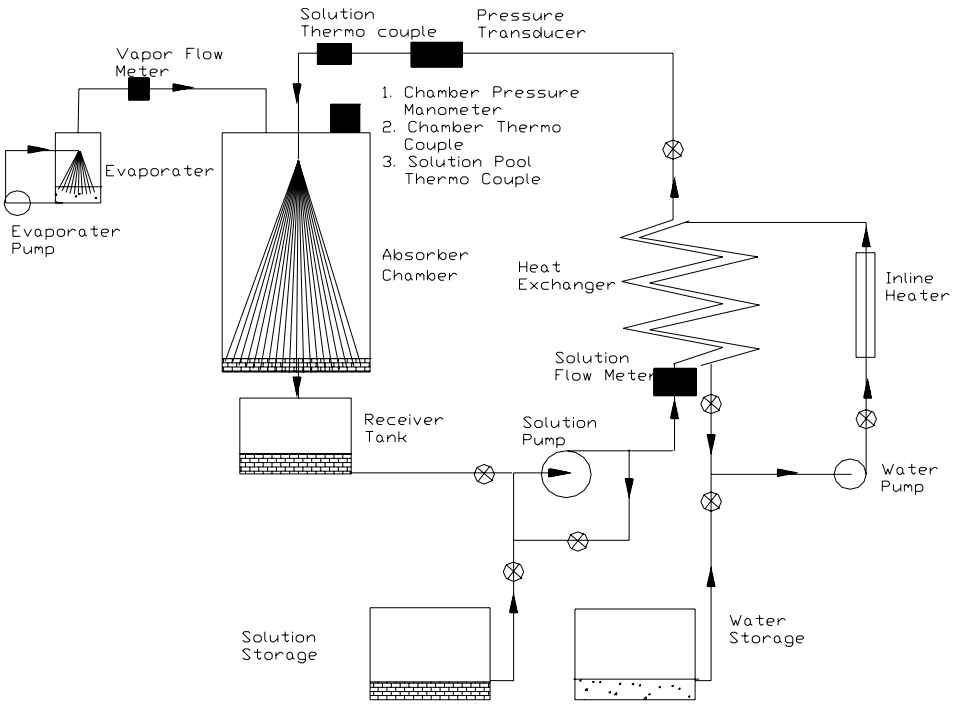

Fig. 3. Schematic diagram of experimental test setup.

the ''Newman'' absorption model were calculated. Then, for each nozzle tested, the experimental and model results were compared. Finally, the nozzles that are suited for industrial applications and their optimum performance parameters are established.

6. Uncertainty analysis

The uncertainties associated with the results of this experiment are primarily caused by instrumentation error and operating error. The instrumentation error, which is due to the accuracy, repeatability and calibration of instruments, affected the experimental results. The operating error caused by the variation of parameters such as properties of the solution and the operating conditions also introduced error into the experimental results.

The error analysis used the root mean square method of the form

$$\text{RMS error} = \sqrt{\sum \left[\Delta \left(\frac{\partial \rho}{\partial \Delta} \right) \right]^2}. \tag{19}$$

The RMS errors calculated for both experimental and model results related to each nozzle are given in Tables 3

Table 3
RMS total of error percentages on experimental results

Error source	Error	Percentage effect on the results					
		SJ1 [%]	SJ2 [%]	SJ2W [%]	SJ3 [%]	FJ [%]	FJW [%]
Instrument error							
Nozzle temperature	0.45 F	1.6	1.7	2.3	2.2	2.0	2.4
Pool temperature	0.55 F	1.6	1.8	2.4	2.3	2.0	2.5
Nozzle pressure	0.25%	2.5	2.4	1.4	2.3	9.4	1.9
Chamber pressure	0.1 mbar	1.3	1.4	1.1	1.7	2.3	1.6
Solution flow rate	0.2% flow	0.9	1.4	1.1	1.7	1.5	1.2
Heater resistance	0.05 Ω	2.5	2.9	1.5	3.3	1.6	1.6
Evaporator current	0.02 amp	1.1	1.4	1.1	1.7	1.0	1.0
Vapor flow rate	0.15%	5.7	7.4	4.9	9.5	5.4	5.4
Operating error							
Solution concentration	0.1%	3.2	3.6	3.8	3.7	3.0	3.0
Solution density	0.2%	4.6	4.8	3.5	5.0	3.2	3.2
Solution viscosity	0.3%	5.3	5.8	4.4	6.1	4.2	3.9
Latent heat of water	1.2%	0.1	0.1	0.1	0.2	0.0	0.1
RMS total of all errors		8.0	8.1	6.9	8.4	7.8	8.4

Table 4
RMS total of error percentages on model results

Error source	Error	Percentage effect on the results					
		SJ1 [%]	SJ2 [%]	SJ2W [%]	SJ3 [%]	FJ [%]	FJW [%]
Instrument error							
Nozzle temperature	0.45 F	1.8	1.8	1.7	2.5	2.0	2.2
Pool temperature	0.55 F	1.8	1.8	2.3	2.6	2.9	2.5
Nozzle pressure	0.25%	2.6	2.5	1.6	2.4	10.7	2.0
Chamber pressure	0.1 mbar	1.3	1.5	1.6	1.6	2.3	1.8
Solution flow rate	0.2% flow	0.9	1.4	1.1	1.7	1.5	1.2
Drop size	–	–	–	–	–	–	–
Drop speed	–	–	–	–	–	–	–
Distribution factor	–	–	–	–	–	–	–
Chamber length	0.1 in.	0.5	0.5	0.5	0.5	0.5	0.5
Spray angle	3°	6.6	5.3	7.9	4.5	8.6	10.0
Operating error							
Solution concentration	0.1%	3.6	3.8	3.9	3.5	3.4	3.2
Solution density	0.2%	4.8	5.3	4.0	5.1	3.7	4.8
Solution viscosity	0.3%	5.4	6.0	4.6	6.4	4.4	4.3
Fourier time number	0.21	2.3	2.6	1.7	2.8	4.5	1.8
Peclet number	0.07	1.3	1.5	1.1	1.6	1.1	1.2
RMS total of all errors		10.0	10.3	13.0	11.1	8.4	10.6

and 4 and error bars based on the percentages are indicated on the results shown in Figs. 4–9.

7. Results and discussion

The selection of nozzles for the experiment was crucial. When selecting nozzles, the flow rates, drop sizes generated, velocity of drops and operating pressures were considered. From the experimental results obtained for the nozzle flows under fully developed and controlled flow conditions with the salt solution, the ranges of performance are given in Table 5.

The experimental and model absorption results for the swirl-jet (SJ), full-jet (FJ) and its wide-angle nozzles tested are shown in Figs. 4–9. The plots given in Figs. 4–9 are drawn by linearly correcting the absorption ratio due to small difference in chamber pressure (i.e., typically ± 0.0025 kPa).

In general, these results show the effect of the degree of sub-cooling and the solution flow rate on the absorption process. The results for most of the nozzles show a slight increase in the absorption ratio (i.e., the amount of water vapor absorbed by a unit amount of solution sprayed) as the flow rate increases. This is a very desirable feature in absorption equipment, since the flow rate of such machines will be much higher than that for the experimental absorber. When comparing the absorption performance, the results show that the swirl-jet nozzles performed better than any other nozzles tested. In spite of increases in the nozzle pressure, the spray angle increased only slightly.

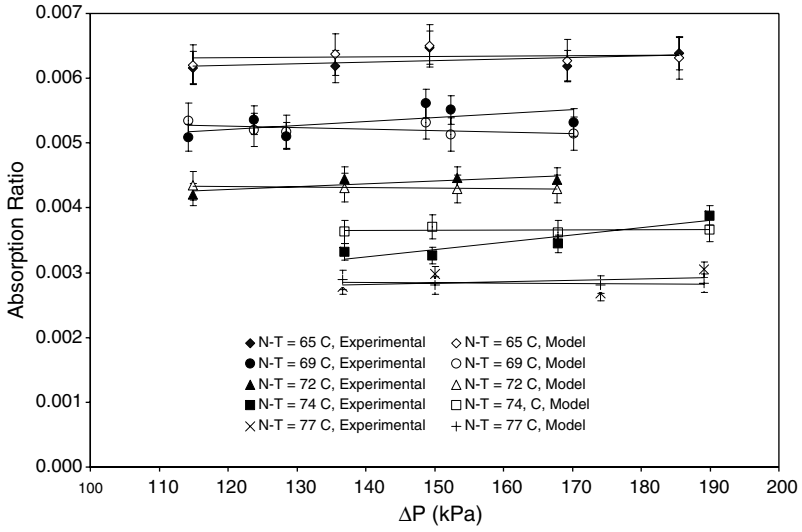

Fig. 4. Comparison of experimental and model absorption results of 1/8 BX SS 1 (SJ1).

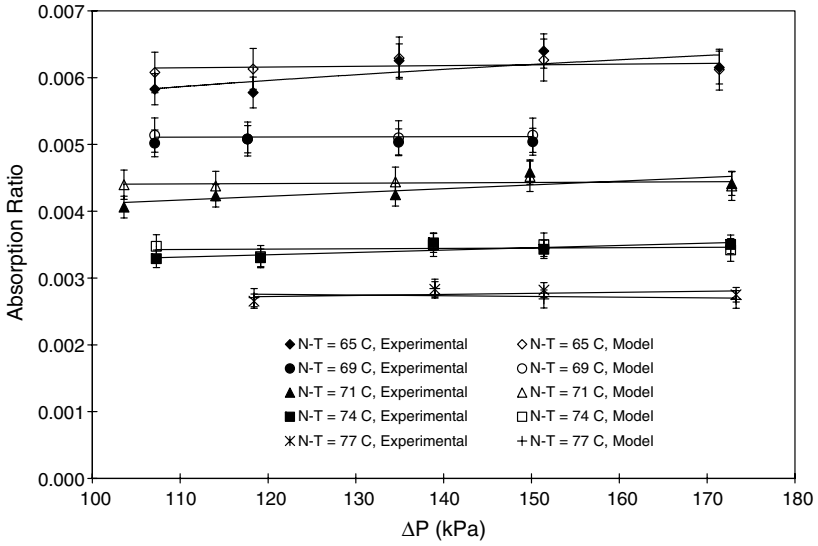

Fig. 5. Comparison of experimental and model absorption results of 1/8 BX SS 2 (SJ2).

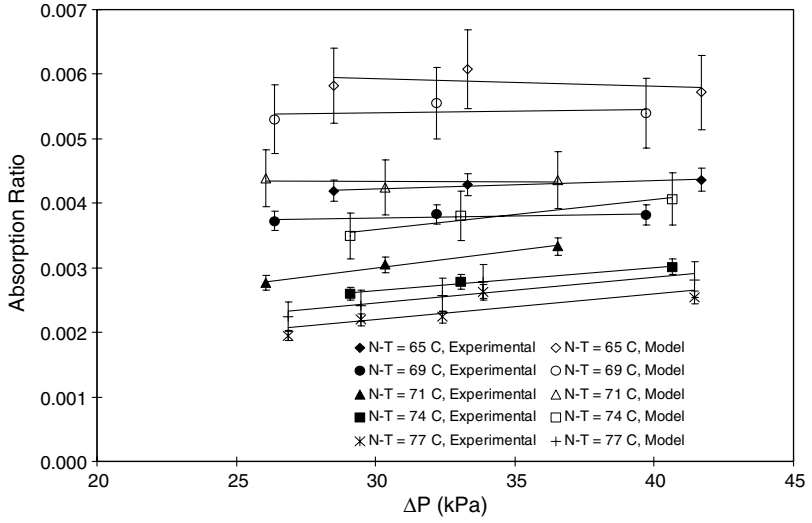

Fig. 6. Comparison of experimental and model absorption results of 1/8 BX SS 2W (SJ2W).

For industrial applications, this is a very good attribute, since it allows limiting the diameter of the absorber chamber. Based on this observation, operating swirl-jet nozzles at their maximum capacity seems practical and more economical.

The calculation of model absorption results is based on the Newman absorption model [6] discussed previously. In general, for all the nozzles at all the sub-cooled conditions, there is relatively good agreement between experimental results and the Newman absorption model. The difference between the experimental and predicted results shows a slight deviation for low flow rates, but as the flow rate increases, this difference becomes negligible. In addition, as the level of sub-cooling decreases, the model predicts the absorption rate decreases proportionally. However, the experimental results show that the reduction of absorption ratio is not as significant.

In the case of nozzle pressure, the experimental absorption ratio increases with nozzle pressure, where the model predicts lower absorption ratios. The reason for this difference is the model only considers the drop quality of an individual drop (size and velocity), but not the drop quantity (flow rate). That is when the nozzle pressure increases, in parallel to the drop size and drop speed, the number of drops leaving the nozzle increases. This, which is reflected in the experimental results, is not taken into account in the model. Further, the increase of the size and the speed is larger than predicted.

For wide-angle nozzles, there is a clear difference between the experimental and model results. The reason being that when running experiments with wide-angle nozzles, free dripping of fairly large droplets can be observed through the view port in the test chamber. This is because the wide-angle nozzles "infinitely" expand the

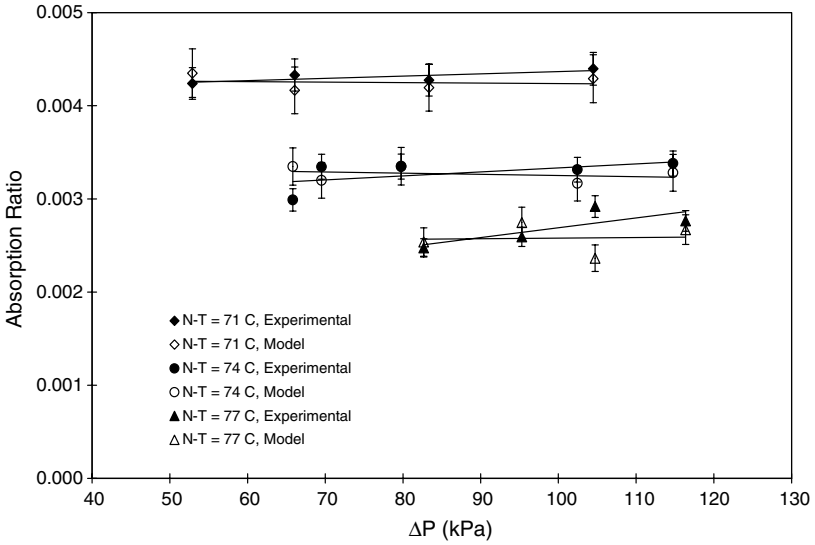

Fig. 7. Comparison of experimental and model absorption results of 1/8 BX SS 3 (SJ3).

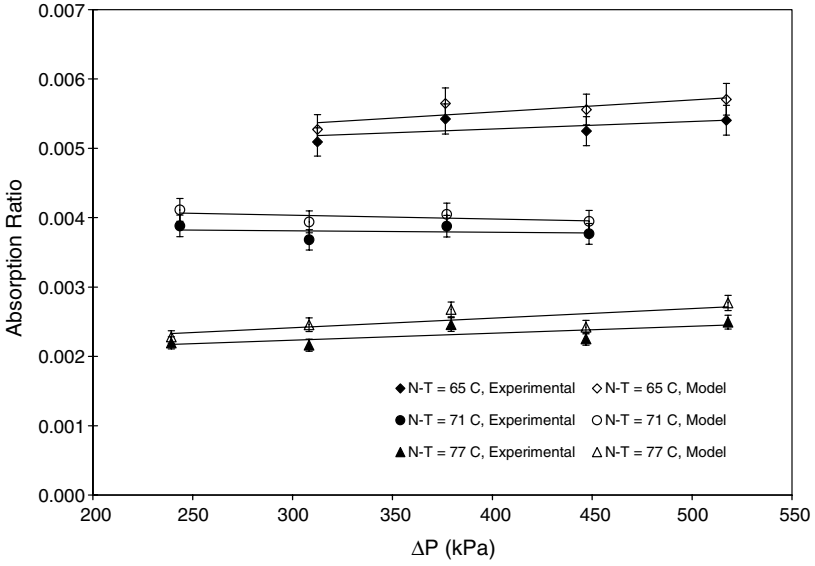

Fig. 8. Comparison of experimental and model absorption results of 1/8 GG SS 2 (FJ).

flow suddenly in the absorber under sub-atmospheric conditions. In this case, due to the limitation of the chamber diameter, the nozzle pressure was kept low. This caused a considerable portion of the flow to drip as big droplets from the nozzle and those large drops having poor absorption properties due to the smaller surface area per unit volume. However, the model results over predict the performance, since it was based on a drop scan through the PDPA measurement system, which scans only drops passing through the measurement volume, was unable to measure the impact of the large drops. Therefore, the absorption ratios predicted by the model are comparatively higher than the experimental results, as shown in Figs. 6 and 9.

In the case of regular full jet nozzles, the nozzle pressures corresponding to fully developed sprays are very high. Therefore, the solution pumping power requirements, one of the major obstacles to use of spray absorption techniques, will be very high and this type of nozzle is not economically feasible [17].

In addition to the above factors governed by the solution spray flow, increasing the absorber pressure can increase the rate of absorption. When absorber pressure increases, the difference between the solution spray vapor pressure and the equilibrium water vapor pressure of the solution becomes greater. This promotes the absorption of the water vapor to the solution droplets. When designing the spray absorbers for commercial applications,

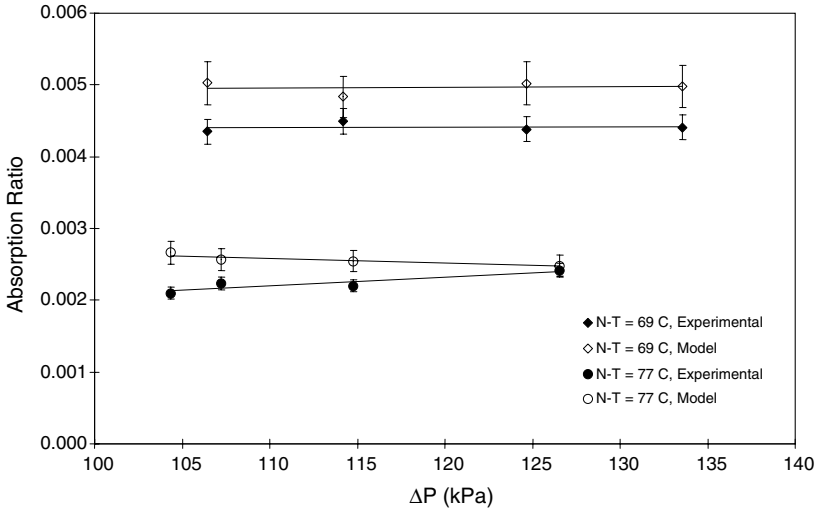

Fig. 9. Comparison of experimental and model absorption results of 1/8 GG SS 2.8W (FJW).

Table 5
Nozzle performance with proprietary salt solution

Nozzle	Pressure range (gauge), P [kPa (psig)]	Flow rate range, Q [kg/s (lb_m/min)]	Mean drop velocity range, V [m/s]	Drop diameter range, MVD [μm]
1/8 BX SS 1 (SJ1)	14.8–90 (2.15–13.05)	0.018–0.025 (2.40–3.27)	8.85–11.74	373–411
1/8 BX SS 2 (SJ2)	3.5–73 (0.51–10.6)	0.027–0.034 (3.61–4.49)	9.81–12.52	387–420
1/8 BX SS 2W (SJ2W)	(78.6)–(57.5) ((11.41)–(8.33))	0.019–0.024 (2.53–3.22)	5.21–11.06	383–469
1/8 BX SS 3 (SJ3)	(47.2)–16.4 ((6.84)–2.37)	0.031–0.043 (4.15–5.72)	9.85–12.93	384–423
1/8 GG SS 2 (FJ)	139.3–419.65 (20.19–60.82)	0.013–0.019 (1.66–2.52)	12.43–16.44	417–485
1/8 GG SS 2.8W (FJW)	0.76–33.5 (0.11–4.85)	0.025–0.029 (3.31–3.79)	10.70–12.37	459–480

optimization of nozzle elevation and optimization of drop density is very important.

8. Conclusions

Drop size, which controls the surface area available to absorb water vapor, is a very important parameter. However, the experimental drop size is 20% larger than expected due to the effect of surface tension on drop formation, which is larger than predicted. From the experimental results, it can be seen that the increasing of sub-cooled levels lead to increase the absorption. However, increasing the sub-cooled level or decreasing the temperature of the solution spray, increases the viscosity that greatly reduces the drop size. Therefore, the sub-cooled level does not affect the experimental absorption rate as was predicted. The experimental results show the effect of the viscosity on drop size is not significant as predicted. The viscosity only affects the spray angle and hence the resident time of the droplets in the absorption chamber. Increasing the chamber height can eliminate this disadvantage. Therefore, in applications, the designer can obtain the maximum use of sub-cooled condition.

Concentration change across a drop and hence F, the fractional approaches to equilibrium is proportional to Pe number and k^{-1}. In the experiment, the solution drops falling through the vacuum has very high viscosity ratio, k and it reduces the absorption. In addition, due to the low Pe number, the internal circulation within the drop will also be very low. However, for small drops, even a small amount of internal circulation within the drop brings a dramatic effect to the absorption rate. On the other hand, when the diameter of drop increases, the surface area decreases and it will adversely affect the absorption rate. However, as the diameter increases, internal circulation increases enhancing the absorption rate. Since these two effects have opposite affect on the adsorption rate, caution has to be taken when designing equipment.

When the drop speed increases, the resident time of the drops decreases and it decreases the absorption rate. However, as the drop speed increases, the Reynolds number increases, causing an increase in drop circulation. These

also are counteracting effects and designer must take precautions to make the net effect positive.

Results given in Figs. 5 and 8 for swirl and full jet nozzles with similar configurations shows that the swirl jet nozzle worked better under these experimental conditions due to the reasons discuss in the above section.

Due to the nature of the sprayed salt solution and the flow configurations, the assumptions that made to select the theoretical model seems are valid and the predicted results closely match the experimental results as are shown in Figs. 5–9.

Acknowledgements

Financial, special, material and technical support given for this work by the Institute of gas Technology, the Gas Research Institute (now the Gas Technology Institute) and the Trane Company is gratefully acknowledged.

References

[1] A. Benbrahim, M. Prevost, R. Bugarel, Performance of a composite absorber, spraying and falling film, in: Proceeding of the International Workshop on Research Activities on Advanced Heat Pumps, Institute of Chemical Engineering, Graz, Austria, October 1986.
[2] M. Flamensbeck, F. Summerer, P. Riesch, F. Ziegler, G. Alefeld, A cost effective absorption chiller with plate heat exchanger using water and hydroxides, Appl. Thermal Eng. 18 (1998) 413–425.
[3] I. Morioka, M. Kiyota, A. Ousaka, T. Kobayashi, Analysis of steam absorption by a sub-cooled droplet of aqueous solution of LiBr, JSME Int. J., Ser. II 35 (1992) 458–464.
[4] W. Ryan, Water absorption in an adiabatic spray of aqueous lithium bromide solution, Ph.D. Thesis, Illinois Institute of Technology, Chicago, 1995.
[5] Trane Company, Dhuring diagram and enthalpy chart for proprietary new absorbent use in multi-effect cycle chillers, 1996.
[6] A.B. Newman, The drying of porous solids, diffusion and surface emission equations, AIChE J. 27 (1931) 203–220.
[7] R. Higbie, The rate of absorption of a pure gas in to a still liquid during short periods of exposure, AIChE J. 31 (1935) 365–389.
[8] R. Kronig, J.C. Brink, On the theory of extraction from falling droplets, J. Appl. Sci. Res. A 2 (1950) 143–154.
[9] A.E. Handlos, T. Baron, Mass and heat transfer from drops in liquid–liquid extraction, AIChE J. 3 (1957) 127–136.
[10] P. Rose, R. Kintner, Mass transfer from large oscillating drops, AIChE J. 12 (1966) 530–534.
[11] N.I. Grigor'eva, V.E. Nakoryakov, combined heat and mass transfer Dhuring absorption in drops and films, J. Eng. Phys. 32 (1976) 243–247.
[12] N.I. Grigor'eva, V.E. Nakoryakov, Exact solution of combined heat and mass transfer Dhuring film absorption, J. Eng. Phys. 32 (1977) 1349–1353.
[13] E. Ruckenstein, Mass transfer between single drop and a continuous phase, Int. J. Heat Mass Transfer 10 (1967) 1785–1792.
[14] R. Clift, J. Grace, M. Weber, Bubbles, Drops and Particles, Academic Press, Harcourt, Brace, Jovanovich, 1978.
[15] F.S.K. Warnakulasuriya, Spray absorption application for multi-effect absorption cycles, M.S. Thesis, University of Illinois at Chicago, Chicago, IL, 1998.
[16] G. Grossman, Simultaneous heat and mass transfer in film absorption under laminar flow, Int. J. Heat Mass Transfer (10) (1967) 1785–1792.
[17] F.S.K. Warnakulasuriya, Heat and mass transfer and water absorption properties of new absorbent droplets, Ph.D. Thesis, University of Illinois at Chicago, Chicago, IL, 1999.